ChemComm

COMMUNICATION

View Article Online
View Journal

Facile synthesis of nanostructured $CuCo_2O_4$ as a novel electrode material for high-rate supercapacitors†

Cite this: DOI: 10.1039/c3cc48773c

Received 17th November 2013,
Accepted 16th December 2013

DOI: 10.1039/c3cc48773c

www.rsc.org/chemcomm

Afshin Pendashteh,[a] Mohammad S. Rahmanifar,[b] Richard B. Kaner[c] and Mir F. Mousavi*[ac]

$CuCo_2O_4$ nanostructures were synthesized through a facile solution combustion method. Electrochemical investigations demonstrate a novel electrode material for supercapacitors with remarkable performance including high-rate capability, high-power density (22.11 kW kg^{-1}) and desirable cycling stability at different current densities.

With demand growing every day for electric energy storage for electrical vehicles and portable devices, electrochemical capacitors or supercapacitors (SCs) have stimulated extensive research interest due to their high-power density, high-rate capability and long cycle life.[1] The charge storage mechanism in SCs is based on either non-Faradaic electrochemical double layer capacitance (EDLC) or fast, reversible Faradaic redox reactions (pseudocapacitance).[2] Transition metal oxides have been extensively investigated as pseudocapacitive materials due to their potentially higher capacitance compared to EDLCs, mainly ascribed to their multiple oxidation states.[3] However, they suffer from intrinsically low electrical conductivity and the fact that fast Faradaic reactions only occur at the surface of the electrode.[4] These disadvantages hinder their application in high-rate supercapacitors. Therefore, novel materials or strategies to improve the performance of the electrode materials for high-power applications, including fabrication of nano-engineered structures or utilizing synergistic effects of hybrid materials, are needed.[5,6] Among the many transition metal oxides, Co_3O_4 has been widely studied in pseudocapacitors, and has demonstrated promising performance.[7] Complete or partial substitution of Co with low-cost and benign elements to form the spinel structure could prove to be even better.[8] Recently, $CuCo_2O_4$ nanostructures have been investigated as an anode material in Li-ion batteries, showing high Li-ion storage capacities,[8,9] suggesting that they can offer high-charge storage capacity through redox reactions.

In this communication, a simple urea combustion method is combined with a post annealing process to synthesize nanostructured $CuCo_2O_4$ particles in the shape of cauliflower-like structures. The electrochemical behavior of the sample as a novel material for supercapacitor electrodes was evaluated using different electrochemical techniques including cyclic voltammetry (CV), chronopotentiometry (CP), and electrochemical impedance spectroscopy (EIS).

$CuCo_2O_4$ nanostructures were synthesized *via* a combustion route using the corresponding nitrate salts as precursors and urea as fuel. The detailed preparation procedure can be found in the ESI.† Moreover, a sample comprised of $CuCo_2O_4$ microparticles was also synthesized *via* the co-precipitation method (see ESI†).

The as-prepared samples were structurally characterized by means of powder X-ray diffraction (XRD). The XRD patterns of both samples can be entirely indexed to a cubic spinel copper cobaltite structure with the lattice parameter a = 8.039 Å, belonging to the *Fd3m* space group (Fig. 1a, and Fig. S4A, ESI†), which is well matched with the JCPDS file no. 001-1155. These features are also in good agreement with previous reports.[8,9] For clarity, the *hkl* lines are ascribed to the corresponding peaks. Broadened diffracted peaks for the nanostructured sample illuminate the fine crystalline size of the

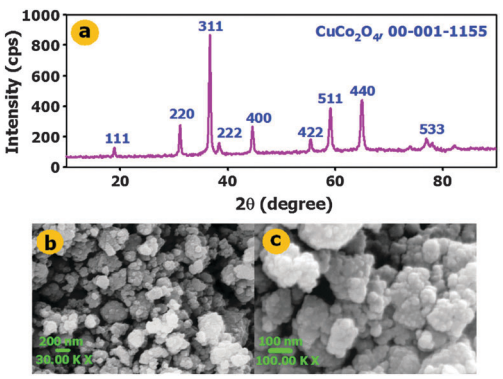

Fig. 1 XRD pattern (a), and FESEM of $CuCo_2O_4$ nanostructures magnified 30 000× (b) and 100 000× (c).

[a] Department of Chemistry, Tarbiat Modares University, Tehran, Iran
[b] Faculty of Basic Sciences, Shahed University, Tehran, Iran
[c] Department of Chemistry and Biochemistry and California NanoSystems Institute, University of California, Los Angeles (UCLA), Los Angeles, CA 90095, USA. E-mail: mousavim@modares.ac.ir, mousavi@chem.ucla.edu

† Electronic supplementary information (ESI) available: Details of the experimental procedure. See DOI: 10.1039/c3cc48773c

sample, which has been further confirmed with a crystallite size of 7 nm calculated using the Debye–Scherer equation (see ESI†).

Field emission scanning electron microscopy (FESEM) was employed to explore the morphology of the prepared samples. As can be seen in Fig. 1b and c, the nanostructured sample is comprised of irregular cauliflower-like microstructures with segregated particles. A highly magnified image (Fig. 1c) shows that the microstructures are themselves composed of fine nanoparticles, mostly with size distribution ranging from 20–30 nm (Fig. S1, ESI†) with a calculated average size of 28 nm. The sample synthesized *via* co-precipitation is comprised of agglomerated particles, mostly 100 nm in size (Fig. S4B, ESI†).

Energy dispersive X-ray (EDX) analysis was performed to obtain bulk compositional characterization of the sample. The corresponding spectrum (Fig. S2, ESI†) reveals that the sample does indeed consist of copper and cobalt with a molar ratio of Cu/Co = 0.491, consistent with the formula $CuCo_2O_4$.

Nitrogen (N_2) adsorption–desorption experiments were performed for the surface characterization and pore structure analysis of the samples (isotherms are shown in Fig. S3A, ESI†). Accordingly, a specific surface area of 13.5 $m^2\ g^{-1}$ was calculated using the BET method. The pore size distribution was also obtained by BJH analysis (Fig. S3B, ESI†), showing that a significant proportion of the pores are centered around 3.72 nm.

The electrodes were prepared using $CuCo_2O_4$ micro and nanostructures applied on Ni foam (see ESI†) to explore their electrochemical behavior in a three-electrode configuration using 3 M KOH as the electrolyte. Fig. 2 shows the cyclic voltammograms (CVs) of the bare electrode (Ni foam) and $CuCo_2O_4$ nanostructures at a scan rate of 5 mV s^{-1}. The non-rectangular shape of the CV curve indicates that Faradaic reactions are responsible for charge storage making this material a pseudocapacitor. The pairs of redox peaks observed originate from Faradaic reactions related to Co^{4+}/Co^{3+} and Cu^{2+}/Cu^{+} associated with OH^- anions. The CV measurements were also conducted at different scan rates ranging from 5 to 100 mV s^{-1} (Fig. S5, ESI†). Increasing the scan rate increases both the magnitude of the current and the potential peak separation, mainly due to polarization and Ohmic resistance during the Faradaic process. The linear relationship between the square root of the scan rate and the anodic peak currents (Fig. S6, ESI†) reveals that the reaction kinetics followed during the redox reactions are likely controlled by diffusion of OH^- anions.

Galvanostatic charge–discharge measurements were performed at current densities between 1 and 50 A g^{-1} to evaluate the application

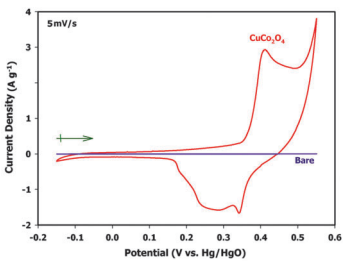

Fig. 2 CV of the bare Ni foam (current collector) and the as-prepared $CuCo_2O_4$ electrode at a scan rate of 5 mV s^{-1}.

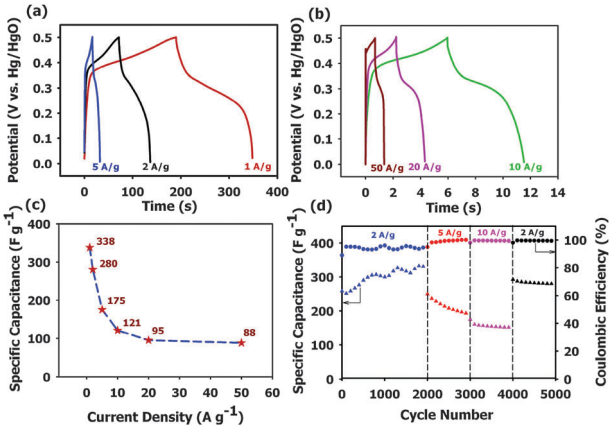

Fig. 3 Galvanostatic charge–discharge curves (a, b), rate capability (c); cycling performance and coulombic efficiency of $CuCo_2O_4$ nanostructures at different current densities (d).

of $CuCo_2O_4$ nanostructures as pseudocapacitor materials. As can be seen in Fig. 3a and b, the obtained profiles are far from the linear charge–discharge curves characteristic of EDLCs, indicating pseudocapacitance behavior resulting from electrochemical adsorption–desorption or redox reactions at the electrode–electrolyte interface. The specific capacitance values calculated from the charge–discharge tests are 338, 280, 175, 121, 95, and 88 F g^{-1} at current densities of 1, 2, 5, 10, 20, and 50 A g^{-1}, respectively. In order to give a better representation, the specific capacitance values *vs.* current densities are depicted in Fig. 3c, which, after increasing the current density by a factor of 50, still shows a capacitance of 88 F g^{-1} (about 26% retention). This suggests a very good capacitive performance for the nanostructured $CuCo_2O_4$ particles under very high current density operation conditions (typically here 50 A g^{-1}) which is significant in practical supercapacitor applications. The maximum capacitance obtained for the micro sample was calculated to be about 42 F g^{-1}, 8 times smaller than that obtained for $CuCo_2O_4$ nanoparticles, which decreases to 8 F g^{-1}, about 19% retention, at 50 A g^{-1}. This can be attributed to the fact that the nanostructured characteristic of the material with segregated particles permits better permeation of the electrolyte and therefore reducing the diffusion time of OH^- ions as well as providing more accessible sites for redox reactions.[10] Accordingly, most of the $CuCo_2O_4$ nanostructures efficiently participate in the redox reactions even at high discharge current densities. The capacitance loss at extreme current densities is mainly due to a contribution of the Ohmic drop (ESR) and sluggish kinetics of the redox couples in $CuCo_2O_4$ at high current densities.

Capacitance retention over prolonged charge–discharge cycles is essential for practical supercapacitor materials. Therefore, charge–discharge tests up to 5000 cycles at different current densities were performed to evaluate the cyclability of $CuCo_2O_4$ nanostructures (Fig. 3d). A clear enhancement in the specific capacitance is observed during the first 2000 cycles at a current density of 2 A g^{-1}. After 1800 cycles, the specific capacitance reached an almost constant capacitance of 320 F g^{-1} (more than a 20% increase). This observation is likely due to structural activation and pore opening of the sample during cycling.[10,11] For the next 1000 cycles, the

measurement was continued at a current density of 5 A g^{-1}. The specific capacitance decreased to 77% of its initial value of about 250 F g^{-1} after 1000 cycles. Upon increasing the current density to 10 A g^{-1}, the sample retained about 86% of its capacitance over the next 1000 cycles, reaching a capacitance of 151 F g^{-1}. After 4000 continuous cycles at successively increased current densities, the capacitance recovered to 293 F g^{-1} when the current density was turned back to 2 A g^{-1}. The next 1000 cycles exhibited good stability with about 96% capacitance retention. These observations demonstrate excellent cycling performance of $CuCo_2O_4$ nanostructures at different current densities. The columbic efficiency (CE) of the sample during 5000 continuous cycles can also be seen in Fig. 3d. During the initial cycles, the efficiency was about 90% which increased to 95% by the end of the first 2000 cycles. Gradually, the CE increased up to 99.5% in the 5000th cycle. The increase in CE, and achieving such high efficiencies, indicates excellent reversibility of the material during charge–discharge, confirming the structural activation of the material during cycling and providing more accessibility and mass diffusion for the interfacial reactions.

In order to demonstrate the overall performance of the $CuCo_2O_4$ nanostructured material, a Ragone plot (specific power *vs.* specific energy) is shown at various current densities, with comparisons to recently reported nanostructures of Co_3O_4 with high-performance (Fig. 4a, Table S2, ESI†). As can be seen, $CuCo_2O_4$ delivers a high power density of 22.11 kW kg^{-1} at an energy density of 3.05 W h kg^{-1}.

To our knowledge, the power density obtained here is higher than all of the reported values for Co_3O_4, except for the ultra-layered structures reported by Rao *et al.* that benefit from a special morphology obtained through a hydrothermal route in the presence of a surfactant. Moreover, one of the highest obtained power density values for CuO is also shown in this figure, indicating a power density of about 1.715 kW kg^{-1} (ESI,† ref. S5) which is far lower than the value obtained for $CuCo_2O_4$. All of these results suggest that $CuCo_2O_4$ is a good candidate for use as the active material in high-rate supercapacitors. Despite the high-power characteristics of this material, it should be noted that the energy density of the material still needs to be improved to be comparable with other well-known supercapacitor materials, such as Co_3O_4 and $NiCo_2O_4$.[6,10]

In order to further investigate the electrochemical behavior of $CuCo_2O_4$ nanostructured materials, EIS measurements were performed at open circuit potential before and after cycling. Fig. 4b shows a Nyquist plot for $CuCo_2O_4$ electrodes before and after 2000 cycles at a current density of 2 A g^{-1}. As can be seen, a semicircle appears in the high frequency region, showing some resistance during charge transfer at the solid oxide/liquid electrolyte interface. The linear part at lower frequencies originates from diffusive resistance of the OH^- anions from the bulk solution to the oxide surface and also within the oxide pores. The experimental data were analyzed through a CNLS fitting method based on Randles equivalent circuit (ESI,† Fig. S7 and Table S1). In the proposed circuit, ESR, R_{ct}, W, CPE1, and CPE2 refer to equivalent series resistance, Faradaic charge transfer resistance, Warburg impedance, double layer capacitance, and bulk Faradaic pseudo-capacitance, respectively. The CPE can be obtained using the following equation:[12]

$$Z_{CPE} = T_{CPE}(j\omega)^{-n} \quad (1)$$

where T_{CPE} and n refer to the CPE coefficient and exponent, respectively, while ω represents the angular frequency. The CPE exponent, n, ranges from −1 to 1. Accordingly, for $n = -1$, 0, 0.5, and 1, the CPE is equivalent to a pure inductor, a pure resistor, diffusive behavior, and a pure capacitor, respectively.

Clearly, the ESR showed an increase from 0.970 to 1.263 Ω after cycling. Moreover, the charge transfer resistance increased after cycling from 6.575 to 23.12 Ω, indicating that the diminished Faradaic reaction may be due to the loss of adhesion of some of the active material within the current collector during the charge–discharge cycling. The linear part at the lower frequencies became steeper after cycling (phase elements, n, has increased from 0.816 to 0.846 for CPE1 and from 0.929 to 0.998 for CPE2, ESI,† Table S1), which shows facilitated ionic diffusion and more access to the electrolyte. Also, the double layer capacitance is increased. This is possibly due to structural activation and pore opening of the sample during cycling.[10]

In conclusion, a facile solution combustion method was used to synthesize cauliflower-shaped nanostructured $CuCo_2O_4$ particles, and electrochemical measurements demonstrate their application as a novel electrode material for high-rate SCs. The material exhibits a high capacitance of 338 F g^{-1} at 1 A g^{-1} (8 times greater than that obtained with $CuCo_2O_4$ microparticles) and even shows a capacitance of 88 F g^{-1} at an extremely high current density of 50 A g^{-1}, with high power density of 22.11 kW kg^{-1}. Moreover, the electrochemical stability and cycling performance of the material for 5000 continuous cycles at various current loads demonstrates the electrochemical suitability of $CuCo_2O_4$ as a promising electrode material for high-rate SC applications.

This work was financially supported by Tarbiat Modares University Research Council.

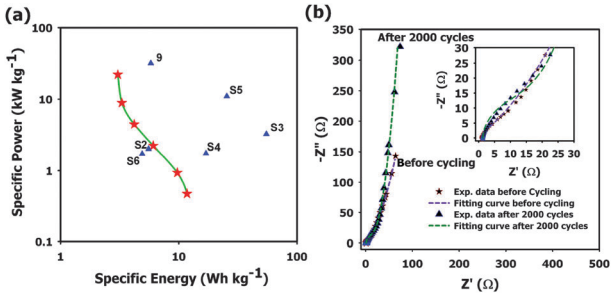

Fig. 4 Ragone plot for $CuCo_2O_4$ nanostructures at different current densities (1–50 A g^{-1}) in comparison to some previous reports with their maximum reported values plotted (a), numbers refer to the references and S refers to ESI;† a Nyquist plot of the sample before and after cycling (b).

Notes and references

1 M. F. El-Kady, V. Strong, S. Dubin and R. B. Kaner, *Science*, 2012, **335**, 1326–1330; G. Zhang and X. W. Lou, *Sci. Rep.*, 2013, 3, DOI: 10.1038/srep01470.
2 H. R. Ghenaatian, M. F. Mousavi and M. S. Rahmanifar, *Synth. Met.*, 2011, **161**, 2017–2023; P. Simon and Y. Gogotsi, *Nat. Mater.*, 2008, **7**, 845–854; H. R. Ghenaatian, M. F. Mousavi and M. S. Rahmanifar, *Electrochim. Acta*, 2012, **78**, 212–222.

3 A. Pendashteh, M. S. Rahmanifar and M. F. Mousavi, *Ultrason. Sonochem.*, 2014, **21**, 643–652; W. Deng, X. Ji, Q. Chen and C. E. Banks, *RSC Adv.*, 2011, **1**, 1171–1178; X. Lang, A. Hirata, T. Fujita and M. Chen, *Nat. Nanotechnol.*, 2011, **6**, 232–236; X. Pan, Y. Zhao, G. Ren and Z. Fan, *Chem. Commun.*, 2013, **49**, 3943–3945; A. Pendashteh, M. F. Mousavi and M. S. Rahmanifar, *Electrochim. Acta*, 2013, **88**, 347–357.
4 X. Wang, X. Han, M. Lim, N. Singh, C. L. Gan, M. Jan and P. S. Lee, *J. Phys. Chem. C*, 2012, **116**, 12448–12454; X. Wang, B. D. Myers, J. Yan, G. Shekhawat, V. Dravid and P. S. Lee, *Nanoscale*, 2013, **5**, 4119–4122.
5 R. B. Ambade, S. B. Ambade, N. K. Shrestha, Y.-C. Nah, S.-H. Han, W. Lee and S.-H. Lee, *Chem. Commun.*, 2013, **49**, 2308–2310; J.-Y. Kim, K.-H. Kim, S.-B. Yoon, H.-K. Kim, S. H. Park and K. B. Kim, *Nanoscale*, 2013, **5**, 6804–6811; K. Naoi, W. Naoi, S. Aoyagi, J.-i. Miyamoto and T. Kamino, *Acc. Chem. Res.*, 2012, **46**, 1075–1083.
6 G. Zhang and X. W. Lou, *Adv. Mater.*, 2013, **25**, 976–979.
7 X.-h. Xia, J.-p. Tu, Y.-q. Zhang, Y.-j. Mai, X.-l. Wang, C.-d. Gu and X.-b. Zhao, *RSC Adv.*, 2012, **2**, 1835–1841; L. Zhuo, Y. Wu, J. Ming, L. Wang, Y. Yu, X. Zhang and F. Zhao, *J. Mater. Chem. A*, 2013, **1**, 1141–1147.
8 M. V. Reddy, C. Yu, F. Jiahuan, K. P. Loh and B. V. R. Chowdari, *RSC Adv.*, 2012, **2**, 9619–9625.
9 Y. Sharma, N. Sharma, G. V. S. Rao and B. V. R. Chowdari, *J. Power Sources*, 2007, **173**, 495–501.
10 S. K. Meher and G. R. Rao, *J. Phys. Chem. C*, 2011, **115**, 15646–15654.
11 B. Senthilkumar, K. Vijaya Sankar, R. Kalai Selvan, M. Danielle and M. Manickam, *RSC Adv.*, 2013, **3**, 352–357.
12 M. E. Orazem and B. Tribollet, *Electrochemical impedance spectroscopy*, Wiley. com, 2011.

